PLOS | ONE

Low-Cost Motility Tracking System (LOCOMOTIS) for Time-Lapse Microscopy Applications and Cell Visualisation

Adam E. Lynch   , Junian Triajianto, Edwin Routledge

Abstract

Direct visualisation of cells for the purpose of studying their motility has typically required expensive microscopy equ
However, recent advances in digital sensors mean that it is now possible to image cells for a fraction of the price of
microscope. Along with low-cost imaging there has also been a large increase in the availability of high quality, ope
analysis programs. In this study we describe the development and performance of an expandable cell motility syste
inexpensive, commercially available digital USB microscopes to image various cell types using time-lapse and perfc
assays in proof-of-concept experiments. With this system we were able to measure and record three separate assa
simultaneously on one personal computer using identical microscopes, and obtained tracking results comparable ir
from other studies that used standard, more expensive, equipment. The microscopes used in our system were capa
maximum magnification of 413.6×. Although resolution was lower than that of a standard inverted microscope we fc
difference to be indistinguishable at the magnification chosen for cell tracking experiments (206.8×). In preliminary (
experiments using our system, velocities (mean μm/min ± SE) of 0.81±0.01 (*Biomphalaria glabrata* hemocytes on ι
1.17±0.004 (MDA-MB-231 breast cancer cells), 1.24±0.006 (SC5 mouse Sertoli cells) and 2.21±0.01 (*B. glabrata* hc
Poly-L-Lysine coated plates), were measured and are consistent with previous reports. We believe that this system
open-source analysis software, demonstrates that higher throughput time-lapse imaging of cells for the purpose of :
can be an affordable option for all researchers.

Data Availability: The authors confirm that all data underlying the findings are fully available without restriction.
data are within the paper and its Supporting Information files.

Competing interests: JR is an independent consultant coder unaffiliated with a university or research departme
not alter the authors' adherence to PLOS ONE policies on sharing data and materials.

Introduction

Cell motility has become an integrated measure used in a variety of modern assays spanning many research discip
cells, individually or as groups, are vital to biological processes including fertilisation, growth and differentiation, imr
progression of diseases, such as cancer [1]–[3]. Consequently, a number of systems for studying motility are availa
researchers and practitioners. For example, Trans-well assays (such as the Boyden chamber) enable measuremen
in response to a chemical stimulus (chemotaxis). Chemotactic responses are quantified by the extent to which cells
across a porous membrane towards a chosen test chemical [4]. However, despite being a relatively inexpensive me
measuring motility Trans-well assays do not permit direct observation of cells as they move [4], [5].

Direct visualisation is considered to be the 'gold-standard' in motility studies, enabling precise and continuous meas
speed, trajectory and morphology of individual cells under a microscope [6]. Cell motility is recorded by equipping th

with a digital camera and acquiring pictures at specific intervals over a chosen period of time (time-lapse) [1]. Howe experiments often take several hours, and possibly days, to complete making these a daunting and laborious task v single microscope is available.

Over the last couple of decades, there have been considerable technological advancements in microscopy hardwar to enable a large degree of automation over time-lapse studies [7], [8]. These advances include motorised stages a auto-focusing software which together allow the acquisition of images across numerous samples without the need f intervention [8]. A basic commercial setup for performing motility studies usually requires an inverted microscope, d software and an incubator/heated stage and would be expected to cost several thousand pounds (GBP) whereas m systems can reach several hundred thousand pounds [9], [10]. Due to high software and hardware costs such syste accessible only to those with large budgets, and are often outside the reach of non-specialist researchers, or those countries with fewer resources [7]. Indeed, affordable solutions for the direct visualisation of cells is rapidly becomin area in its own right [11]–[14].

The recent ability to produce low-cost imaging devices is a consequence of improvements in image sensors such a coupled devices (CCDs) and complementary metal oxide semiconductors (CMOS) enabling good quality imaging to substantial decreases in size and cost [13]. Such devices are now produced for a range of applications from diseas [14] to measurement of sperm motility [15]. However, although these can vastly increase the affordability of motility deliver high image quality, none can match the high-throughput nature of the more expensive devices. Therefore, th low-cost imaging will be to develop solutions to increase their throughput ability.

Along with advances in hardware, recent years have also seen a significant increase in the amount of high quality c software (which in many cases is comparable in capability to commercial packages) written for the analysis of micro Here we show that by combining a number of low-cost imaging devices with open-source software we are entering high-throughput digital microscopy imaging can be an affordable option for all researchers. Building on existing wor imaging, we hope that this system will help make motility measurements accessible to all researchers, and inspire c continue to enhance the productivity of similar devices.

Materials and Methods

Construction

The design process (Figure 1A) began by creating a 3D model of the system in Trimble Sketchup 8 (Figure 1B). Th constructed using oak, the stage from acrylic and the microscope support bases were created from adjustable kitch which fit them well and allow the height to be adjusted so that the top of the microscope is level with the stage and s prevents image drift and allows for optimum magnification (Figure 1C). Detailed information regarding the construct be found in supporting information (Protocol S1, Protocol S2, Figure S1, Figure S2 and Table S1).
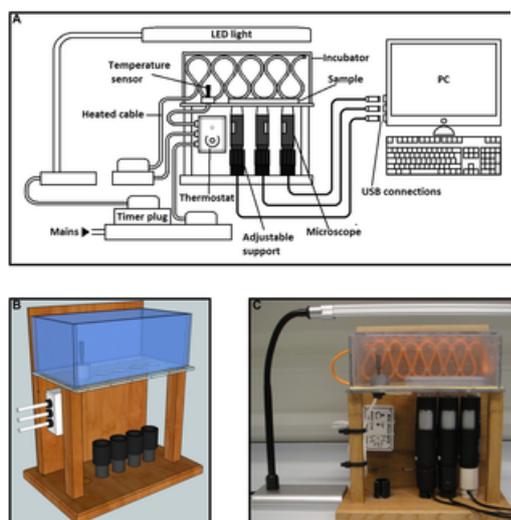

Figure 1. Images of the microscope system.
(a) Schematic diagram of microscope system; (b) CAD model; (c) Photograph of finished system.
doi:10.1371/journal.pone.0103547.g001

Microscopes

All three microscopes used were identical models (VMS-004D, Veho, Hampshire, UK) in order to prevent any discre microscopes use a CMOS image sensor with 1.3 mega-pixel resolution (2 MP with interpolation, although interpola used in our studies). Magnification has two set levels (~20× minimum and ~400× maximum) achieved using a focus enhance stability, magnification and to allow for observation of live samples in liquid (cells) the microscopes were in

Lighting

Various lighting sources were tested, and ultimately an LED strip desk lamp was selected. The microscopes' inbuilt turned off. LEDs were used due to their low heat emission and intensity which helps reduce stress to the cells. To fu the risk of phototoxicity an accurate timer plug was used to turn the light off between image capturing. It was import light source which could be adjusted since different samples have different requirements (due to depth or transpare

Heating

In order to keep samples at a constant physiological temperature, without needing to place the whole system inside an incubation chamber was developed to fit over the top of the stage. The chamber was made from transparent acr visualisation inside. The edges of the chamber were fitted with foam to improve insulation and the chamber was se stage using metal clips. The heating element used was a 37.5 w soil warming cable; this was chosen since it is eco waterproof and highly flexible. To maintain a constant temperature the heating cable was connected to a commercia thermostat of the kind typically used to heat vivariums (MicroClimate Ministat 100). The stability of the incubator ten measured at 27°C by placing a 'Tinytag' data logger (Gemini Data Loggers, Chichester, West Sussex, UK) inside w programmed to take temperature measurements every minute for 20 hours.

Resolution

The ultimate definition of resolution is described as the minimum distance two objects can be separated by and still distinguished as separate features; this is sometimes referred to as spatial resolution. Spatial resolution is therefore important quantitative measurement. It is important to note that in digital systems spatial resolution is also related to dependent on, pixel resolution which refers to the number of pixels utilised to create the image (width×height). In th imaging systems it is therefore also necessary to consider pixel resolution, as this can determine the amount of info the real object that is retained within the digital image. If the number of pixels used to create the image is too low in [18],[19].

Pixel resolution in Autokams was set at 640×480. Although the microscopes are capable of higher resolution, time- typically generate a large number of files. Therefore, given the fact that three cameras were running together, a low resolution was chosen to reduce memory demand and enhance system stability. Spatial resolution was tested using solution of latex beads with a mean particle size of 1 μm (Sigma-Aldrich) trapped between two cover-slips.

Magnification and Horizontal field of view

The calculation of digital image magnification is dependent on a number of factors and differs to those used in optic due to the lack of eye pieces and the fact that objects are viewed on a screen. Determining the magnification of an screen is dependent on knowing the PPI (pixels per inch) of the screen, the size of a single pixel on the screen, the image in pixels and the actual size of the object being magnified (Figure S3). Pixel resolution is also an important fa determining 'useful' magnification as, up to a point, more pixels mean that the image contains more information whi observable to the eye when it is enlarged. Simply put, magnification is used to make viewing easier, but if informatio in the image increased magnification will not show any more detail [18].

Horizontal field of view (HFOV) and full magnification were measured using a calibration slide with a 1 mm marker a subdivisions. The lower magnification and HFOV were measured with a 15 cm ruler with 1 mm subdivisions.

Software

Image capture.

The microscopes are bundled with native image capture software, however, due to the unique requirements of this necessary to write a custom application. 'AutoKams' is a standalone application designed to capture images from U devices, such as web cams and microscopes (Figure 2). It was developed using Microsoft Visual Studio 2010 with (programming language. The application is powered by AForge.NET framework (http://www.aforgenet.com/). In mar identical USB devices (such as our three microscopes) are connected to the same PC they conflict as the compute identify them uniquely, this leads to the PC crashing, or the display of only a single camera. Although some devices in tandem, this was not the case with any of the microscope models we tested. Autokams was written to allow for th capture of multiple USB devices of the same model when running on a machine with multiple USB controllers. Imag time-lapse studies were typically captured every 60,000 milliseconds for 1 hour using the capture control box and a saved to labelled folders. Our software is open-source, licensed under LGPL v3, and can be downloaded at: http://l /AutoKams. The software was tested for stability on several Windows PCs, altered accordingly, and was shown to b with three different models of USB microscope (400× maximum magnification, 8 LED, 2 MP interpolated CMOS). T described here remained stable throughout all our experiments.
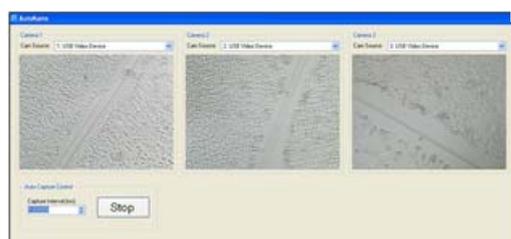
Figure 2. Autokams software interface.
Three separate scratch assays of MDA-MB-231 cells displayed simultaneously on Autokams.
doi:10.1371/journal.pone.0103547.g002

Image preparation and analysis.

Image preparation and analysis was performed within the open-source Java-based image processing program Ima
version 1.44). To set the precise scale an image of an object of known distance was uploaded, then, using the 'set s
corresponding size in pixels could be set and applied to other objects. Experimental images (Figure 3A) were loade
converted to 8-bit (Figure 3B). Uneven illumination often occurs in microscope images and is difficult to eliminate co
this reason the images were also subject to the 'subtract background' tool (Figure 3C). The stack was then threshol
binary image with better contrast between cells and background (Figure 3D). The final stage of image preparation w
any minor drift that may occur; this was achieved using the 'image stabilizer' plug-in [17]. To analyse cell motility the
'MTrack2' by Nico Stuurman was used (Figure 3E). Minimum track length was set at 10 frames. Although there was
chemoattractant used we also analysed the same data using the ImageJ chemotaxis tool by Gerhard Trapp as an e
further applications (Figure 3F).
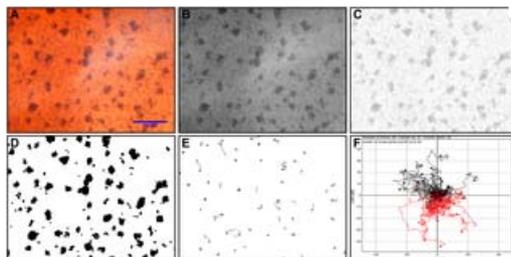
Figure 3. Analysis process in ImageJ.
(a) Original image; (b) 8-bit black and white; (c) Background subtraction; (d) Thresholded; (e) MTrack2 cell trajec
Chemotaxis plot.
doi:10.1371/journal.pone.0103547.g003

Assays

Cell tracking.

Cell tracking was performed on cells from three different species: primary hemocytes (immune cells) from the fresh
Biomphalaria glabrata, mouse juvenile Sertoli cells (SC5) [20] and human breast cancer epithelial cells (MDA-MB-2
B.glabrata were maintained in our laboratory in flow-through tanks at 27°C with a 12 hour light and dark cycle and f
commercial fish flakes. Sterile *B.glabrata* hemolymph was collected according to Fryer and Bayne (1995) [22] and c
diluted 50% in snail saline (CBSS PH 7.4; Chernin, 1963 [23]) and allowed to settle for 30 minutes at 27°C before ti
began. *B.glabrata* hemocytes were prepared in two separate conditions; cells were either left to attach to the plate c
onto a surface of 0.01% poly-L-lysine according to Boehmler *et al.* (1996) [24] with some minor modifications. Both
MDA-MB-231 cells were seeded into wells of a 96-well plate in phenol red-free DMEM medium (10% fbs, 1% Gluta
penicillin-streptomycin - Sigma Aldrich) and allowed to reach approximately 20–30% confluence. The mammalian c
37°C during imaging. All time-lapse images were taken every minute for 1 hour.

Scratch assay.

Scratch assays are a very widely used method to investigate wound healing in various cell types [25]. We performe
assays using MDA-MB-231 cells seeded into 3 wells of a 6-well plate to near full confluence using the same culture
cell tracking. Scratches were made in each well using the tip of a sterile scalpel. Each well was positioned over a se
microscope, and the thermostat was set to 37°C. Images were captured every 4 minutes from each camera over a
hours.

Artemia development.

The effectiveness of the microscope for imaging three very different samples simultaneously was tested using shrin
genus *Artemia*, as they are a common test organism and developmental stages are clearly distinguishable. Cysts w
from ZM foods (Winchester, UK) and were cultured in 20% salinity at 28°C. Samples from different life stages were
separate wells of a 6-well plate or placed on a microscope slide and imaged at the two different magnifications.

Statistical analysis.

Analysis was performed on the MTrack2 data generated from the time-lapse files included in supporting information
S3 and S4). As the data failed to meet all the assumptions of an ANOVA and was not amenable to transformation a
test was performed in SPSS version 20 (IMB) to determine whether recorded velocity values differed significantly fc
cell types. As a post-hoc test pairwise comparisons were performed using Dunn's procedure with a Bonferroni corre
multiple comparisons (Figure S4).

Results

Microscope Functional Parameters

Heating stability.

After approximately 1 hour the desired temperature (27°C) was achieved (Figure 4). After the first hour the tempera
by more than 0.5°C either side of this temperature for the remaining 19 hours although a gradual increase could be
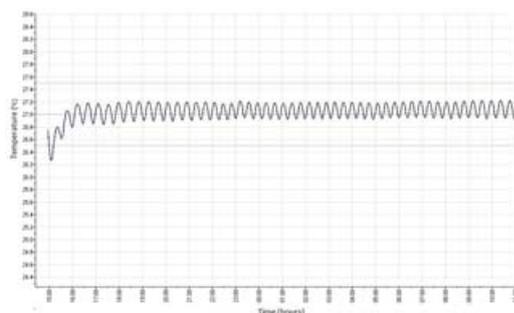

Figure 4. Incubator temperature stability over time.
Incubator temperature readings (°C) taken every minute for 20 hours.
doi:10.1371/journal.pone.0103547.g004

Field of view and magnification.

Based on the calibration slide, the horizontal field of view at maximum magnification was determined to be 0.99 mm
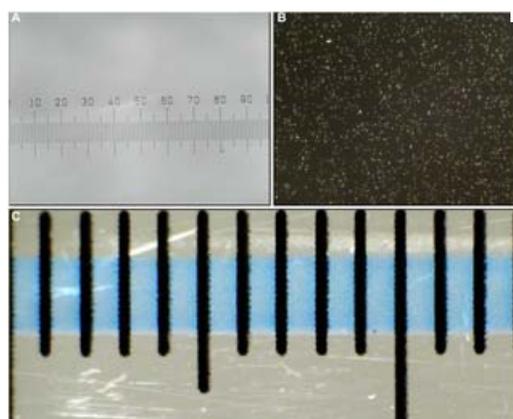and 13 mm for the lower magnification (Figure 5 C) at 640×480.

Figure 5. Calibration images.
(a) 1 mm graticule with 10 µm subdivisions at 206.8× magnification; (b) 1 µm latex beads at 206.8× magnificatio
ruler at 15.7× magnification with 1 mm subdivisions.
doi:10.1371/journal.pone.0103547.g005

We estimated the maximum magnification at the pixel resolution chosen for cell tracking (640×480) to be 206.8× or
PPI of 78 and the lower magnification to be 15.7× (Figure S3). This calculation appears accurate when we enlarge
with our microscope by 149% (the percentage difference in size between 206.8× and an image taken at the same p
on a conventional inverted microscope at 310×, (Figure 6 A and B)). The microscopes are capable of greater magn
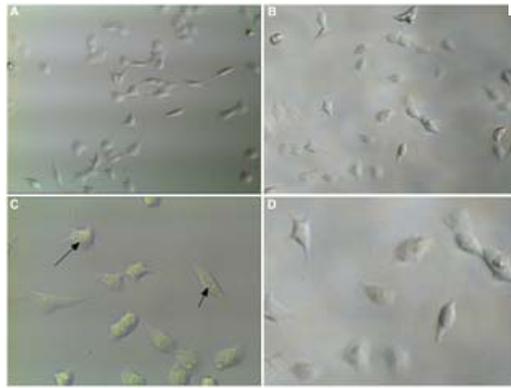resolution is set to the maximum of 1280×960.

Figure 6. Comparison of MDA-MB-231 cell images between our system and a conventional optical microscope.
(a) 310× image taken at 640×480 with a conventional inverted microscope; (b) 206.8× image taken at 640×480 with our system and enlarged post acquisition by 149% to match the size; (c) 620× image taken at 1280×960 with a conventional inverted microscope, arrows show intra-cellular detail; (d) 1280×960 image taken with our system at full magnification (413.6×) and enlarged post-aquisition by 149% to match the size.
doi:10.1371/journal.pone.0103547.g006

Pixel resolution.

The improvement in image quality when increasing pixel resolution from 640×480 to 1280×960 was found to be minimal at the magnification used for cell tracking (Figures 7A and C) but doubles the file size (and therefore storage requirements). This only becomes apparent when the images are increased significantly in size post-acquisition, a noticeable increase in quality can be seen when enlarging an image taken at 640×480 by 800%, which is the same on-screen size as an image taken at 1280×960 enlarged by 400% (Figures 7B and D), however these sizes are far in excess of what would be useful for our purposes.
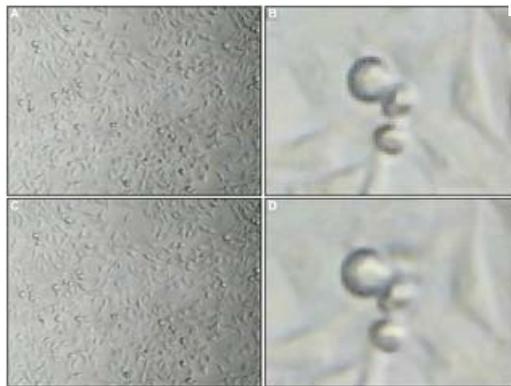

Figure 7. Comparison of digital microscope pixel resolutions between 640×480 and 1280×960.
(a) 640×480 image at full magnification; (b) 640×480 image enlarged post-acquisition to 800%; (c) 1280×960 image at full magnification reduced in size by 50%; (d)1280×960 image enlarged post-acquisition to 400%.
doi:10.1371/journal.pone.0103547.g007

Spatial resolution.

At full magnification, 10 µm divisions were clearly visible and 1 µm beads were distinguishable. However, the measured size of the beads was larger than 1 µm suggesting that the microscope was picking up the reflected light (Figure 5B). Spatial resolution was therefore determined to be at least 10 µm. Crucially we were able to clearly resolve all cell types tested (size range 10–40 µm) and we could distinguish individual cells from one another and from the background.

Comparison with a conventional microscope.

The imaging capability of our system was compared to a conventional inverted microscope (GX XDS-3) fitted with a digital camera. The highest magnification on the conventional microscope (620×) was greater than our system (413.6×), with resolution of images was the same (1280×960). Spatial resolution on the conventional microscope was higher and intra-cellular detail could be seen at the highest magnification that could not be distinguished in our system when images were enlarged to match the size (Figure 6 C and D). Images can be enlarged post-acquisition, or by using interpolation, to increase detail but this results in 'empty magnification' and it resolves no more detail than the original image while resulting in substantial loss of quality (Figure 7 A and B). When comparing the two systems using lower magnification and pixel resolution (as was used for motility tracking assays) we can see little difference in the quality of the images and both would be equally suitable for motility

6 A and B). Finally, the cost of assembling our system was approximately £161, whereas a conventional inverted m camera) retails for approximately £3,250 (Table S1).

Lighting.

In order to achieve optimum resolution and improve signal-to-noise ratio (SNR) the in-built LED lights were turned c that for most cell samples optimum SNR was achieved from an external overhead light source (Figure 8).
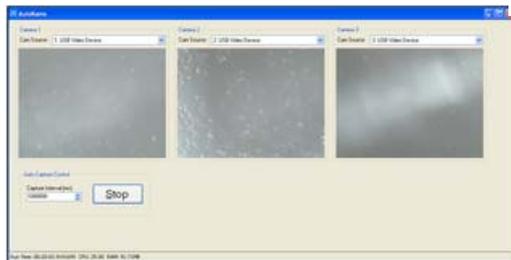

Figure 8. Autokams interface showing the result of illumination from the in-built LEDs alone.
doi:10.1371/journal.pone.0103547.g008

Applications

Cell velocity.

According to visual inspection, the Kruskal-Wallis test distributions of velocity scores were not similar for all groups and velocity values differed significantly between cell types, χ^2 (3) = 106.531, p = >.001 (see Figure S4 A–C). Pairw comparisons showed significantly lower velocity of spread *B.glabrata* cells (0.81±0.01 µm/min; Figure 9, Movie S4) other cell types, including *B.glabrata* on PLL (2.21±0.01 µm/min; Figure 9, Movie S1). There were significant differe between MDA-MB-231 cells (1.17±0.004 µm/min; Figure 9, Movie S2) and both *Biomphalaria* cell culture methods, (1.24±0.006 µm/min; Figure 9, Movie S3). Likewise, the velocity of SC5 cells differed significantly from both *Biomph* methods but not from MDA-MB-231 cells (Figure 9). Assumptions of the ANOVA test were most likely not met since accept results from cells of differing track length (between 10–60 tracks).
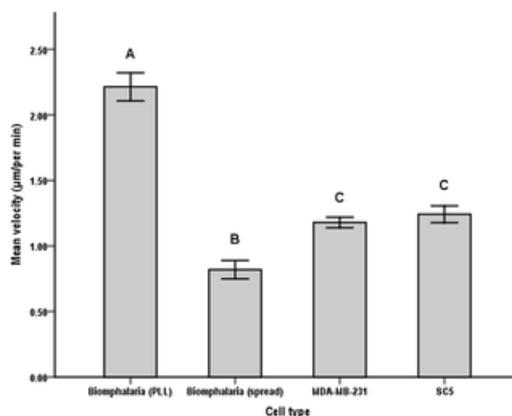
Figure 9. Mean velocity (± SE) in µm per hour of the 4 cell types.
Shared letters indicate no significant difference between cell types according to K-W test pairwise comparisons.
doi:10.1371/journal.pone.0103547.g009

Scratch Assay.

The system was tested for use in performing scratch assays. Not only were the microscopes able to detect cells an sufficient for use in the assay, but it was also found to be relatively simple to align three separate scratches/wells si (Figure 10; Movies S5, S6 and S7). More difficult was keeping each scratch oriented in the same way, but this has r validity of the assay and can easily be altered post-acquisition.

Figure 10. Autokams interface showing individual scratch assays simultaneously recorded on each camera.
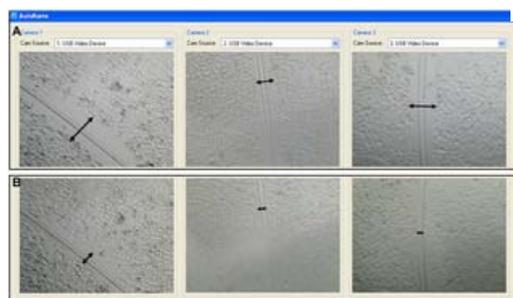(a) cells at 0 hr; (b) cells after 10 hrs; Arrows show the scratch channels.
doi:10.1371/journal.pone.0103547.g010

Artemia development.

We were able to demonstrate the ability of the system to simultaneously image three distinct specimens (Figure 11) was possible to independently alter the magnification of a chosen sample separately. In the case of *Artemia* develo view the smaller life stages (cyst, nauplii) in detail by higher magnification while leaving the much larger adult stage magnification (Figure 11 B).

Figure 11. Ability of the microscope system to image distinct samples in different manners simultaneously.
(a) Cyst, nauplii and adult *Artemia* at 15.7× magnification; (b) Cyst and nauplii at 206.8×, adult at 15.7×; (c) All th 206.8× magnification.
doi:10.1371/journal.pone.0103547.g011

Discussion

In this study we demonstrate the development and application of a low-cost microscope system for multiple time-la inverting commercially available digital microscopes and employing an external light source the stability, working dis signal-to-noise ratio are improved considerably, and images were comparable to a much more expensive standard microscope/camera system. We also show that the system can support a number of microscopes simultaneously, h the throughput capability of time-lapse studies captured onto a single PC. Parallel cell tracking and scratch assays on independent samples with relative simplicity, and the ability of the system to image samples of different sizes sin demonstrated. There was very little difference in the images taken using our system (at maximum magnification wit resolution of 640×480) compared to a conventional inverted microscope at a similar magnification (Figure 6 A and E resolution between the two types of microscope only become apparent when attempting to use higher magnification and D). To achieve the highest useful magnification of the digital microscope (413.6×) the pixel resolution can be se The maximum magnification of the commercial microscope was 620× (although higher objective lenses can be pur 6 C shows an image taken on the conventional microscope at its maximum magnification. As the maximum magnifi on the conventional microscope we needed to enlarge our images post-acquisition in order to make a comparison a Since the limits of the lens and sensor have already been reached for our system this kind of post-acquisition mani example of empty magnification (Figure 6 D). There is considerably greater detail in the image taken with the conve microscope due to its greater spatial resolution. Clearly our system would not be suitable for investigating intracellu perfectly adequate, even at a lower pixel resolution (640×480), for cell tracking. Indeed, greater magnification is not

purpose, especially when factoring the increased cost [25].

A number of published studies now demonstrate the rapidly improving capabilities of digital imaging sensors compa existing standards in microscopy or explore their potential applications[9], [11]–[14], [26]. Despite this, one of the ma many of the lower-cost time-lapse systems is the rate of data collection or 'throughput'. Here we demonstrate the in capability of CMOS sensors to image cells in tandem as an alternative to the expensive systems on a cost-performa the sensors used are small and light weight, it is possible to decrease the size and cost of our system substantially sensors directly from the manufacturer (rather than buying a commercial system sold as a microscope) as these ca as $1.50 a unit [27]. Stripped back sensors would allow more microscopes to fit into a smaller space (for example in pattern) and at much lower-cost. The actual number of microscopes that could be run simultaneously on one PC wc the processor speed, memory (RAM/cache) and the number of available USB ports/controllers. However, given the required for time-lapse studies it is likely that a larger number could be supported. Indeed by sourcing components believe that the three camera system described here could be reproduced for as little as 20 GBP. The ability to run microscopes in tandem actually proved to be one of the biggest challenges in developing this system. The microsco software did not support multiple models and we were unable to find any third-party software that met the criteria. T software platform was written specifically for our requirements, demonstrating the importance of collaboration betwe and programmers; a point that has been stressed by others [2], [28]. We hope that the open-source nature of the sc it to be more widely adopted and adapted for use with other platforms and in communities such as ImageJ and Micr

When performing cell tracking or wound healing assays it is common to render the images post-acquisition to enha (cells) to noise (background and artefact) ratio (SNR), especially when using automated analysis programs. This de beyond a certain point, the overall resolution of the original image has little bearing on the quality of the data [29]. Ir may be unnecessary to invest significant sums of money for high resolution images or high magnification when the be obtained using a less expensive microscope. In the case of cell tracking, high magnification results in a reduced and, consequently, lower sample size and statistical power. Obviously there are conditions where it is crucial to obta information from the image as possible and there is also a minimum level needed to perform tracking assays, espe moving objects. However, in situations where robust motility data is prized above all (attractive images being a sec consideration) there may be little merit in investing large sums of money.

Four different cell types were used to test the ability of the system to measure cell velocity. *B. glabrata* haemocyte c velocity of 0.81 µm/min ±0.01 on an untreated surface, compared to 2.21 µm/min ±0.01 on a poly-L-lysine treated s 9). This is consistent with previous reports of an increase in velocity from 0.99 µm/min ±0.72 (untreated) to 5.13 µm poly-L-lysine coated surfaces using *B. glabrata* haemocytes [24], albeit from a different snail strain. For SC5 cells a velocity of 1.24 µm/min ±0.01 was recorded but we were unable to find sufficient data in the literature for comparisc MDA-MB-231 cells we showed an average cell velocity of 1.17 µm/min ±0.004. There are several existing studies w investigated motility in MDA-MB-231 cells which vary from 0.4–2.5 µm/min[30]–[34], likely due to the variation in ex techniques. Our results are in the middle of this reported range, demonstrating that our system is capable of genera data comparable to those reported in other studies using more expensive equipment.

While the system we have described cannot match the impressive capabilities of the high-end devices needed for la tasks, such as drug discovery, we believe our system would appeal to researchers with limited budgets. In these cir system could be applied to life science education including demonstrations of different stages of development and t exposure conditions in various macro and microscopic organisms (Figure 11). Our system produces results compar inverted microscopes, whilst generating three times the data in a single run. The low memory demands of our syste is likely to be compatible with older machines; for example, we were able to run experiments successfully using a 1 (IBM ThinkCentre 9210). The system is also portable, enabling experiments to be carried out directly in the field.

There are still many areas in which the system could be improved given more time. While the current manual focus works well we believe that this process could be automated by the software in order to reduce the likelihood of acci the field of view while touching the microscope. An important feature which our system currently lacks, but is comm cell culture, is a CO_2 pump. The lack of a CO_2 pump is not believed to have affected the cell tracking experiments s the DMEM media contains CO_2, which would not have depleted in the course of 1 hour [35]. The absence of a CO_2 however, affect longer-term experiments (such as the scratch assay), and this could be addressed by placing the er inside a CO_2 incubator or finding ways to miniaturize the CO_2 supply system. One such design, with the inclusion o CO_2 delivery system, is described by Ho *et al* [36].

Conclusions

In conclusion, we demonstrate the ability of a novel cell tracking system to perform multiple simultaneous time-laps various cell types. Due to its low-cost, portability and commercially available components we believe that this syster potential to enable time-lapse studies by non-specialist departments and schools, and may be a practical solution fo with limited financial resources.

Supporting Information

Figure S1.

Exploded-view. (a) Microscope supports (b) Base plate (c) Support legs (d) Back piece (e) Thermostat (f) Stage (g Incubator (i) Heating cable.

doi:10.1371/journal.pone.0103547.s001
(TIF)

Figure S2.

CAD model of alternative construction plan for microscope housing. (a) 2D plan of stage and incubator (b) 3D assembled unit.
doi:10.1371/journal.pone.0103547.s002
(TIF)

Figure S3.

Magnification equations. Where 'DR' is the diagonal resolution in number of pixels, 'WP' is the Width in pixels, 'HF pixels, 'PPI' is pixels per inch for the specific screen, 'ASP' is the actual size of a pixel in mm, 'DS' is the diagonal s in inches, 'M' is magnification (how many times larger the object on screen is compared to the original), 'IWP' is ima pixels and 'HFOV' is the horizontal field of view at the chosen magnification in mm.
doi:10.1371/journal.pone.0103547.s003
(DOCX)

Figure S4.

SPSS output for Kruskal-Wallis test. (a) Hypothesis test summary (b) Pairwise comparisons of cell type (c) Indep box and whisker plot.
doi:10.1371/journal.pone.0103547.s004
(TIF)

Table S1.

Hardware components and prices.
doi:10.1371/journal.pone.0103547.s005
(DOCX)

Movie S1.

60 minute time-lapse of B.glabrata hemocytes on 0.01% poly-L-lysine surface. AVI file of image stack created converted to 8-bit and stabilized.
doi:10.1371/journal.pone.0103547.s006
(AVI)

Movie S2.

60 minute time-lapse of MDA-MB-231 cells. AVI file of image stack created in ImageJ, converted to 8-bit and stab
doi:10.1371/journal.pone.0103547.s007
(AVI)

Movie S3.

60 minute time-lapse of SC5 mouse Sertoli cells. AVI file of image stack created in ImageJ, converted to 8-bit ar
doi:10.1371/journal.pone.0103547.s008
(AVI)

Movie S4.

60 minute time-lapse of B.glabrata hemocytes spread. AVI file of image stack created in ImageJ, converted to 8 stabilized.
doi:10.1371/journal.pone.0103547.s009
(AVI)

Movie S5.

10 hour scratch assay time-lapse of MDA-MB-231 cells, camera 1. AVI file of image stack created in ImageJ, cc and stabilized.
doi:10.1371/journal.pone.0103547.s010
(AVI)

Movie S6.

10 hour scratch assay time-lapse of MDA-MB-231 cells, camera 2. AVI file of image stack created in ImageJ, cc and stabilized.
doi:10.1371/journal.pone.0103547.s011
(AVI)

Movie S7.

10 hour scratch assay time-lapse of MDA-MB-231 cells, camera 3. AVI file of image stack created in ImageJ, cc and stabilized.
doi:10.1371/journal.pone.0103547.s012
(AVI)

Protocol S1.

Construction method for original microscope system.
doi:10.1371/journal.pone.0103547.s013
(DOCX)

Protocol S2.

Construction method for alternative design.
doi:10.1371/journal.pone.0103547.s014
(DOCX)

References

1. Huth J, Buchholz M, Kraus JM, Schmucker M, von Wichert G, et al. (2010) Significantly improved precision of cell migration analysis ir microscopy through use of a fully automated tracking system. BMC cell biol 11: 24–24. doi: 10.1186/1471-2121-11-24
   View Article • PubMed/NCBI • Google Scholar

2. Meijering E, Dzyubachyk O, Smal I, van Cappellen WA (2009) Tracking in cell and developmental biology. Semin Cell Dev Biol 20: 89∢ 10.1016/j.semcdb.2009.07.004
   View Article • PubMed/NCBI • Google Scholar

3. Hulkower KI, Herber RL (2011) Cell Migration and Invasion Assays as Tools for Drug Discovery. Pharmaceutics 3: 107–124. doi: 10.3390/pharmaceutics3010107
   View Article • PubMed/NCBI • Google Scholar

4. Dai L, Alt W, Schilling K, Retzlik J, Gieselmann V, et al. (2005) A fast and robust quantitative time-lapse assay for cell migration. Exp C 272–280. doi: 10.1016/j.yexcr.2005.09.013
   View Article • PubMed/NCBI • Google Scholar

5. Pujic Z, Mortimer D, Feldner J, Goodhill GJ (2009) Assays for eukaryotic cell chemotaxis. Comb Chem High Throughput Screen 12: 5 10.2174/138620709788681952
   View Article • PubMed/NCBI • Google Scholar

6. Muinonen-Martin AJ, Knecht DA, Veltman DM, Thomason PA, Kalna G, et al. (2013) Measuring Chemotaxis Using Direct Visualizatior Chambers. Methods Mol Biol 1046: 307–321. doi: 10.1007/978-1-62703-538-5_18
   View Article • PubMed/NCBI • Google Scholar

7. Buggenthin F, Marr C, Schwarzfischer M, Hoppe PS, Hilsenbeck O, et al. (2013) An automatic method for robust and fast cell detectio images from high-throughput microscopy. BMC bioinformatics 14: 297–297. doi: 10.1186/1471-2105-14-297
   View Article • PubMed/NCBI • Google Scholar

8. Zanella F, Lorens JB, Link W (2010) High content screening: seeing is believing. Trends Biotechnol 28: 237–245. doi: 10.1016/j.tibtech View Article • PubMed/NCBI • Google Scholar

9. Zimic M, Velazco A, Comina G, Coronel J, Fuentes P, et al. (2010) Development of low-cost inverted microscope to detect early growt tuberculosis in MODS culture. PLoS one 5: e9577–e9577. doi: 10.1371/journal.pone.0009577
   View Article • PubMed/NCBI • Google Scholar

10. Gough AH, Johnston PA (2007) Requirements, features, and performance of high content screening platforms. Methods Mol Biol. 356 10.1385/1-59745-217-3:41
View Article • PubMed/NCBI • Google Scholar

11. Smith ZJ, Chu K, Espenson AR, Rahimzadeh M, Gryshuk A, et al. (2011) Cell-phone-based platform for biomedical device developme applications. PLoS one 6: e17150–e17150. doi: 10.1371/journal.pone.0017150
View Article • PubMed/NCBI • Google Scholar

12. Bishara W, Sikora U, Mudanyali O, Su T, Yaglidere O, et al.. (2011) Handheld and lensless microscope identifies malaria parasites. SF 10.1117/2.1201107.003812. Available: https://spie.org/x51571.xml. Accessed 10th Feb 2014.

13. Kim SB, Koo KI, Bae H, Dokmeci MR, Hamilton GA, et al. (2012) A mini-microscope for in situ monitoring of cells. Lab chip 12: 3976–: 10.1039/c2lc40345e
View Article • PubMed/NCBI • Google Scholar

14. Linder E, Grote A, Varjo S, Linder N, Lebbad M, et al. (2013) On-Chip Imaging of Schistosoma haematobium Eggs in Urine for Diagno Vision. PLoS Negl Trop Dis 7: e2547–e2547. doi: 10.1371/journal.pntd.0002547
View Article • PubMed/NCBI • Google Scholar

15. Su TW, Erlinger A, Tseng D, Ozcan A (2010) Compact and Light-Weight Automated Semen Analysis Platform Using Lensfree on-Chip Chem 82: 8307–8312. doi: 10.1021/ac101845q
View Article • PubMed/NCBI • Google Scholar

16. Patlak M (2010) Open-source science makes headway. J Natl Cancer Inst 102: 1221–1223. doi: 10.1093/jnci/djq321
View Article • PubMed/NCBI • Google Scholar

17. Li K (2008) The image stabilizer plugin for ImageJ. Available: http://www.cs.cmu.edu/~kangli/code/Image_Stabilizer.html.

18. Sellaro TL, Filkins R, Hoffman C, Fine JL, Ho J, et al. (2013) Relationship between magnification and resolution in digital pathology sy Inform 4: 21. doi: 10.4103/2153-3539.116866
View Article • PubMed/NCBI • Google Scholar

19. Brown L (2009) Imaging Particle Analysis: Resolution and Sampling Considerations. Fluid Imaging Technologies, Inc. Available: http://info.fluidimaging.com/resolution-and-sampling-wp. Accessed 8th June 2014.

20. Hofmann MC, Narisawa S, Hess RA, Millán JL (1992) Immortalization of germ cells and somatic testicular cells using the SV40 large Biol 201: 417–435. doi: 10.1016/0014-4827(92)90291-f
View Article • PubMed/NCBI • Google Scholar

21. Cailleau R YR, Olivé M, Reeves WJ Jr (1974) Breast tumor cell lines from pleural effusions. J Natl Cancer Inst 53: 661–674.
View Article • PubMed/NCBI • Google Scholar

22. Fryer SE, Bayne CJ (1995) Cell mediated killing of metazoan parasites by molluscan hemolymph. In: Stolen JS, Fletcher TC, Smith S, Anderson RS, et al.. editors. Techniques In Fish Immunology 4th Ed. Fair Haven, NJ: SOS Publications. 123–131.

23. Chernin E (1963) Observations on hearts explanted in vitro from the snail Australorbis glabratus. J Parasitol 49: 353–364. doi: 10.230'
View Article • PubMed/NCBI • Google Scholar

24. Boehmler AM, Fryer SE, Bayne CJ (1996) Killing of Schistosoma mansoni sporocysts by Biomphalaria glabrata hemolymph in vitro: a hemocyte behavior after poly-L-lysine treatment of plastic, and the kinetics of killing by different host strains. J Parasitol 82: 332–335. 10.2307/3284173
View Article • PubMed/NCBI • Google Scholar

25. Yarrow JC, Perlman ZE, Westwood NJ, Mitchison TJ (2004) A high-throughput cell migration assay using scratch wound healing, a co image-based readout methods. BMC Biotechnol 4: 21–21.
View Article • PubMed/NCBI • Google Scholar

26. Tseng D, Mudanyali O, Oztoprak C, Isikman SO, Sencan I, et al. (2010) Lensfree microscopy on a cellphone. Lab chip 10: 1787–1792 10.1039/c003477k
View Article • PubMed/NCBI • Google Scholar

27. Zheng G, Lee SA, Yang S, Yang C (2010) Sub-pixel resolving optofluidic microscope for on-chip cell imaging. Lab chip 10: 3125–3129. 10.1039/c0lc00213e
View Article • PubMed/NCBI • Google Scholar

28. Cardona A, Tomancak P (2012) Current challenges in open-source bioimage informatics. Nat Methods 9: 661–665. doi: 10.1038/nmet
View Article • PubMed/NCBI • Google Scholar

29. Frigault MM, Lacoste J, Swift JL, Brown CM (2009) Live-cell microscopy - tips and tools. J Cell Sci 122: 753–767. doi: 10.1242/jcs.033
View Article • PubMed/NCBI • Google Scholar

30. Zheng Q, Li X, Sunkara M, Morris AJ, Wu W, et al. (2013) Leptin up-regulates HECTD1 to promote phosphoinositide metabolism and invasion in breast cancer cells. J Pharmacol Clin Toxicol 1: 1001.
View Article • PubMed/NCBI • Google Scholar

31. Wang SJ, Saadi W, Lin F, Minh-Canh Nguyen C, Li Jeon N (2004) Differential effects of EGF gradient profiles on MDA-MB-231 breast chemotaxis. Exp Cell Res 300: 180–189. doi: 10.1016/j.yexcr.2004.06.030
View Article • PubMed/NCBI • Google Scholar

32. Irimia D, Toner M (2009) Spontaneous migration of cancer cells under conditions of mechanical confinement. Integr Biol (Camb)1: 506. 10.1039/b908595e
View Article • PubMed/NCBI • Google Scholar

33. Onuki-Nagasaki R, Nagasaki A, Hakamada K, Uyeda TQP, Fujita S, et al. (2008) On-chip screening method for cell migration genes b transfection microarray. Lab Chip 8: 1502–1506. doi: 10.1039/b803879a
View Article • PubMed/NCBI • Google Scholar

34. Mak M, Reinhart-King CA, Erickson D (2011) Microfabricated physical spatial gradients for investigating cell migration and invasion dy 6: e20825–e20825. doi: 10.1371/journal.pone.0020825
View Article • PubMed/NCBI • Google Scholar

35. Coutu DL, Schroeder T (2013) Probing cellular processes by long-term live imaging-historic problems and current solutions. J Cell Sci doi: 10.1242/jcs.118349
View Article • PubMed/NCBI • Google Scholar

36. Chung-Liang H, Tun-Yi M, Pei-Shuan C, Chu-Li W, Nan-Haw C (2005) Mini chamber system for long-term maintenance and observati Biotechniques 38: 267–273. doi: 10.2144/05382rr03
View Article • PubMed/NCBI • Google Scholar